A comparative study between Piecewise-Linear and Point-Based methodologies for galvanometer mirror systems

Un estudio comparativo entre las metodologías Lineal a Tramos y Basada en puntos para sistemas de espejos galvanométricos

Víctor Manuel Jiménez-Fernández[1], Héctor Vazquez-Leal[1], Uriel Filobello-Nino[1], Héctor H. Cerecedo-Nuñez[2], Patricia Padilla-Sosa[2], Luis Beltrán-Parrazal[3]*

[1] Facultad de Instrumentación Electrónica, Universidad Veracruzana. Circuito Gonzalo Aguirre Beltrán s/n, Zona Universitaria. C.P. 91000. Veracruz, México.

[2] Facultad de Física, Universidad Veracruzana. Circuito Gonzalo Aguirre Beltrán s/n, Zona Universitaria. CP. 91000. Veracruz, México.

[3] Centro de Investigaciones Cerebrales, Universidad Veracruzana. Avenida Dr. Castelazo Ayala s/n, Colonia Industrial Ánimas. CP. 91000. Xalapa, Veracruz, México.

(Received March 28, 2014; accepted July 21, 2014)

Abstract

Galvanometer mirror systems are a fundamental tool used in many research fields to deploy curves over virtually any surface. Even though the point-based methodology is the current standard used to achieve this task, it has the shortcoming of using a format of coordinates (expressed as a massive list of points) to represent the curve to be displayed, requiring large memory arrays. An alternative methodology is the so-called Piecewise-Linear which representation format is based on the use of a mathematical Piecewise-Linear formulation where the curves to be drawn are treated as a parametric system composed of two positional equations, X and Y , related to each other by an artificial parameter μ. In comparison against the point-based method, Piecewise-Linear exhibits attractive advantages such as: memory saving and improved sharpness for projected curves.

----------*Keywords*: Comparative study, piecewise-Linear, point-based, galvanometer mirrors

* Corresponding author: Víctor Manuel Jiménez Fernández, e-mail: vicjimenez@uv.mx

Resumen

Los sistemas de espejos galvanométricos son una herramienta fundamental usada en muchos campos de la investigación para proyectar curvas virtualmente sobre cualquier superficie. Aunque la metodología basada en puntos es el estándar actualmente utilizado para llevar a cabo esta tarea, ésta tiene el inconveniente de usar un formato de coordenadas (expresado como una masiva lista de puntos) para representar la curva a ser proyectada, lo cual requiriere grandes arreglos de memoria. Una metodología alternativa es la denominada Lineal a Tramos cuyo formato de representación se basa en el uso de una formulación matemática Lineal a Tramos donde las curvas a ser dibujadas son tratadas como un sistema de ecuaciones paramétrico compuesto de dos ecuaciones de posición, X y Y, relacionadas una a otra a través de un parámetro artificial μ. Comparado con el método basado en puntos, el método Lineal a Tramos exhibe atractivas ventajas tales como: ahorro de memoria y una mayor nitidez en las curvas proyectadas.

----------*Palabras clave:* Estudio comparativo, Lineal a Tramos, Basado en puntos, espejos galvanométricos

Introduction

Controlled projection of laser beams has becoming common in modern life. Since laser printers and bar-code scanners to manufacturing processes or medical procedures, laser scanning is involved in several aspects of daily life [1-6], hence, several instruments like Scanning Galvanometer Mirror Systems (SGMS) [7, 8] were conceived to systematically control a laser beam projection to reach specific functionalities. This way, it is possible to track the projection across a controlled path to outline a specific pattern. In order to properly project the laser beam, the path must be translated into information the SGMS can follow, toward this, some point-based approaches has been proposed such as the Point-oriented and Vector-oriented methodologies [9, 10]. The first of these methodologies is the actual standard in the laser show industry [11-17] and even when this has proved to be a robust technical standard, it has the disadvantage of using a massive list of points to represent the curve to be displayed what demands the use of big memory banks, even for simple geometric patterns. In an attempt to overcome this problem, Vector-oriented represents the curves into small vectors, significantly reducing the size of the files to be stored at the SGMS [18]. However, if the path of the beam happens to be curve, the amount of vectors can be as big as the number of points of its Point-oriented counterpart. Taking into account all the above, in a recent publication, a new methodology to laser projection has been proposed [19]. Such methodology is based on the use of a mathematical Piecewise-Linear model [20-23] to represent the images to be projected (two-dimensional curves). The proposal uses the decomposed form of the canonical Piecewise-Linear model of Chua-Kang reported in [24-25]. According to this, two functions of the independent variable (parameter) μ, one for each X and Y axes, represent the path that will be followed by the laser beam. With the purpose of gain insight into this alternative, a comparative study between both methodologies, Piecewise-Linear and point-based, is presented. In this study, two aspects have been explored: memory consumption in the curve description and sketching quality.

The Piecewise-Linear Approach

Consider the two dimensional Piecewise-Linear curve depicted in the XY-plane of figure 1. Let this curve be described by L linear segments and (L+1) coordinates collected in the ordered list C={($X1$, $Y1$), ($X2$,$Y2$),..., (XL,YL),(XL+1,YL+1)}

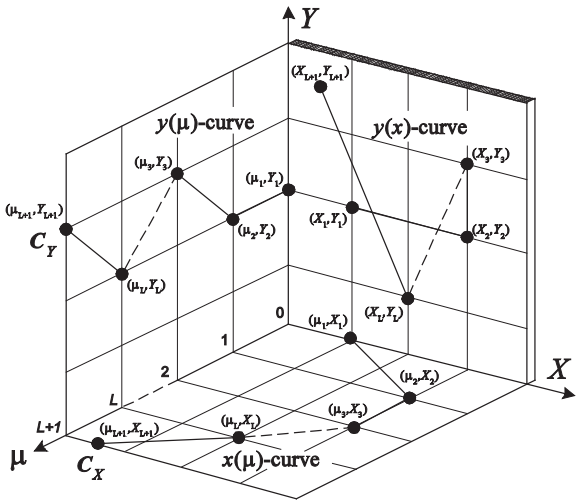

Figure 1 Decomposition of a Piecewise-Linear curve $y(x)$into the parametric system $x(\mu)$-$y(\mu)$

In a traditional Piecewise-Linear analysis, an univalued one-dimensional Piecewise-Linear curve with L segments and σ breakpoints (β_1, β_2, β_3, ..., β_σ), can be described by the explicit function $y(x)$ defined in (1).

$$y(x) = a + bx + \sum_{i=1}^{\sigma} c_i \left| x - \beta_i \right| \tag{1}$$

Where σ=L-1 and $\{a,b,c_i,\beta_i\} \in R^1$ are computed by (2), (3) and (4), respectively.

$$b = \frac{J^{(1)} + J^{(\sigma+1)}}{2} \tag{2}$$

$$c_i = \frac{J^{(i+1)} + J^{(j)}}{2} \tag{3}$$

$$a = y(0) - \sum_{i=1}^{\sigma} c_i \left| \beta_i \right| \tag{4}$$

An alternative form for (1), described in (5) can also be obtained by the algebraic substitution of (4) into (1).

$$y(x) = y(0) + bx + \sum_{i=1}^{\sigma} c_i \left\{ \left| x - \beta_i \right| - \left| \beta_i \right| \right\} \tag{5}$$

As long as the $y(x)$-curve of figure 1 runs from the left most to the right most coordinate, a i-th slope assigned to each linear segment is obtained by (6).

$$J^{(i)} = \frac{Y_{i+1} - Y_i}{X_{i+1} - X_i}, \quad \forall_i = \{1, L\} \uparrow \tag{6}$$

where the notation $i = \{1, L\} \uparrow$ indicates that index i takes the values $\{1,2,..., L\}$ increasing from 1 to n. Thus, it must be noted that due to the strongly dependence on the slope value in the parameter computation, in the case where the condition X_{i+1}=X_i is presented, the $J(i)$-th slope will become infinite what makes it impossible to obtain the mathematical representation in the form of (1) or (5). In order to avoid undefined slope values, the strategy of splitting the list C into two sublists (C_X and C_Y) is adopted as defined in (7) and (8).

$$C_X = \{(0, X_1), (1, X_2), ..., (L-1, X_L), (L, X_{L+1})\} \tag{7}$$

$$C_Y = \{(0, Y_1), (1, Y_2), ..., (L-1, Y_L), (L, Y_{L+1})\} \tag{8}$$

The sketching for these sublists is shown in figure 1, specifically at the μX and μY planes, and their decomposed formulation can be expressed by (9) and (10) as follows:

$$x(\mu) = x_0 + A_x \mu + \sum_{i=1}^{\sigma} B_x^{(i)} \left(\left| \mu - i \right| - \left| i \right| \right) \tag{9}$$

$$y(\mu) = y_0 + A_y \mu + \sum_{i=1}^{\sigma} B_y^{(i)} \left(\left| \mu - i \right| - \left| i \right| \right) \tag{10}$$

where $x_0 = x(0)$ and $y_0 = y(0)$ denote the values of X and Y at μ = 0, and the coefficients A_x and A_y, $B_x^{(i)}$ and $B_y^{(i)}$, $J_x^{(i)}$ and $J_y^{(i)}$, are defined by equations: (11), (12) and (13), respectively.

$$A_x = \frac{J_x^{(1)} + J_x^{(L)}}{2}, \quad A_y = \frac{J_y^{(1)} + J_y^{(L)}}{2} \tag{11}$$

$$B_x^{(i)} = \frac{J_x^{(i+1)} - J_x^{(i)}}{2}, \quad B_y^{(i)} = \frac{J_y^{(i+1)} - J_y^{(i)}}{2} \tag{12}$$

$$J_x^{(i)} = (X_{i+1} - X_i), \quad J_y^{(i)} = (Y_{i+1} - Y_i) \tag{13}$$

for i=$\{1,L\}\uparrow$.

As is can be observed, this model includes an artificial parameter $\mu=\{0,L\}\uparrow$. It is worth mentioning that, due to the non-negative ascendant set of values that the parameter μ takes (from 0 to L), the problem of infinite slopes is overcome. This condition always ensures the capability of achieving a piecewise linear function representation of $y(x)$ into the decomposed form given by (9) and (10), irrespective of whether the curve is open or closed. For further details about the decomposed model of (9) and (10), the reader is referred to [26].

Experiment to Verify the Piecewise-Linear Methodology

Due to the lack of a motor-driver specifically designed for Piecewise-Linear functions, a homemade National Instruments (NI) LabView virtual module was created. This code, shown in figure 2(*a*), interfaces (via the DAQ Assistant) the evaluation results of the Piecewise-Linear functions with the analog outputs AO1 y AO2 in a NI-BNC-2110 card. These analog outputs are connected to the LP-20 galvanometer system [27] in order to provide the signals to control the positions of the galvo mirrors. The Piecewise-Linear equations $x(\mu)$ and $y(\mu)$ are supplied to the virtual instrument in labView following a Block diagram style. It must be noted that the image resolution is directly related to the number of points to be plotted, which is controlled by the α-number of evaluation cycles and the δ-evaluation step size. In figure 2(*a*), the edition of the parametric equation in the formula node box is shown. To illustrate the correct performance of this experimental implementation, the laser projection for a 38 points falcon-icon is shown in figure 2(*b*). Below of this figure, its corresponding decomposed Piecewise-Linear formulation $y(\mu)$, $x(\mu)$ is reported.

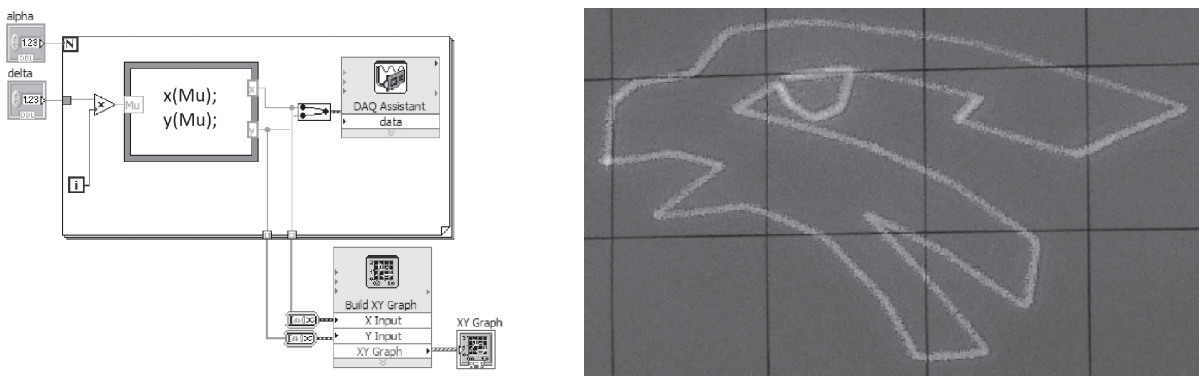

Figure 2 Experimental implementation for the decomposed Piecewise-Linear proposal. (*a*) LabView Front Panel screen in the LP20 galvo system. (*b*) Laser projection for the falcon- icon, α =38, δ =0.1

The decomposed piecewise-linear formulation (expressed in the parametric form of (9) and (10)) for the 38 points falcon-icon is reported in (14) and (15).

$$y(\mu) = -0.2\mu + 9.4 - 0.4125|\mu - 10| - 0.0625\,|\,\mu - 11\,| + 0.5|\mu - 12| - 0.0875|\mu - 14| - 0.05|\mu - 15| - 0.0125|\mu - 16| - 0.0375|\mu - 17| - 0.15|\mu - 18| + 0.0125|\mu - 19| + 0.1125|\mu - 20| + 0.0875|\mu - 21| - 0.125|\mu - 22| - 0.1875|\mu - 25| + 0.125|\mu - 26| - 0.125|\mu - 27| + 0.25|\mu - 28| + 0.275|\mu - 30| - 0.175|\mu - 31| - 0.1625|\mu - 32| - 0.125|\mu - 33| - 0.05|\mu - 35| + 0.125|\mu - 34| - 0.15|\mu - 36| + 0.1375|\mu - 3| - 0.175|\mu - 4| - 0.0875|\mu - 1| - 0.05|\mu - 2| - 0.075|\mu - 5| + 0.025|\mu - 6| + 0.225|\mu - 7| + 0.3375|\mu - 8| - 0.1125|\mu - 9| \quad (14)$$

$$x(\mu) = 0.1875\mu + 0.375|\mu - 10| - 0.15|\mu - 12| + 0.0125|\mu - 14| + 0.0125|\mu - 15| + 0.4|\mu - 17| - 0.1625|\mu - 18| + 0.0625|\mu - 19| + 0.0375|\mu - 20| - 0.05|\mu - 21| - 0.175|\mu - 22| + 0.1375|\mu - 25| - 0.5|\mu - 26| + 0.475|\mu - 27| - 0.225|\mu - 28| - 0.9125|\mu - 30| + 0.15|\mu - 31| + 0.1875|\mu - 32| + 0.175|\mu - 33| + 0.1375|\mu - 35| - 0.075|\mu - 34| + 0.025|\mu - 36| + 0.6375|\mu - 3| - 0.1|\mu - 4| - 0.0875|\mu - 1| - 0.45|\mu - 2| - 0.1|\mu - 5| - 0.0875|\mu - 6| + 0.1875|\mu - 7| - 0.425|\mu - 8| + 0.0375|\mu - 9| + 2.3125 - 0.3375|\mu - 13| - 0.025|\mu - 23| + 0.4|\mu - 24| + 0.1|\mu - 29| \quad (15)$$

Comparative Analysis and Discussion

In this section, a comparative discussion about the performance of the proposed method against the current standard in the laser shows industry (i.e. Point-oriented and Vector-oriented), is presented. Among this discussion, it is important to mention that even when Point-oriented is a technology with high throughput, yields into large files that require big memory arrays to store the massive amount of points to represent a drawing pattern. The above is due to the fact that, in this approach, graphics are defined and stored as a succession of single points. In an attempt to overcome this problem, the Vector-oriented approach represents the graphics into sequence of vectors, which significantly reduce the size of the files to be stored at the SGMS. In contrast, Piecewise-Linear describes a graphic as a set of continuous parametric equations, representing graphics within a smaller file, yielding to reductions in hardware requirements. Furthermore, it must be addressed that while both methods, Point-oriented and Vector-oriented, have a similar file format in which a sequence of point locations or vectors need to be listed, Piecewise-Linear store a single set of two equations which includes all the information needed to sketch the graphic. This characteristic offers the possibility to perform manipulations such as: displacement, scaling, rotation over one or both of their axes (independently or simultaneously), and even more complex operations like animation, this without the need of loading a large amount of additional frames as in Point-oriented or Vector-oriented frameworks. Moreover, in the Point-oriented scheme, graphics are bounded to a specific resolution. Once the resolution is fixed, the whole information contained in the graphic cannot be modified. This leads to several disadvantages, as when the graphic must be displayed with a different resolutions or when it needs to be scaled.

In table 1, a comparison between the file size for the Point-oriented and Piecewise-Linear techniques is summarized. The reference images (Satellite, Cent, and Digital watch of Figure 3) are free images taken from the SpectraScan™ website [28]. As it can be observed, both, the number of points (NOP) and the file size is reduced for the case of Piecewise-Linear. However, the most dramatic difference can be found in the Digital watch pattern (77.78%), whose shape is mainly conformed by straight lines. In contrast, in figures with rounding shapes, like the Cent and Satellite, the memory gain is lesser (16.67% and 10%, respectively). From this, it can be concluded that the better performance of Piecewise-Linear can be found in images mostly composed by straight lines.

Table 1 Comparative between the Point-oriented and the Piecewise-Linear methodologies, memory file size and the number of points (NOP) in each drawing pattern

Image name	*Point-Oriented*		*Piecewise-Linear*		*Gain*	
	Memory	NOP	Memory	NOP	Memory	NOP
Satellite	40 KB	2136 p	36 KB	233 p	10%	1903 p
Cent	6 KB	396 p	5 KB	209 p	16.67%	187 p
Digital watch	27 KB	2039 p	6 KB	175 p	77.78%	1864 p

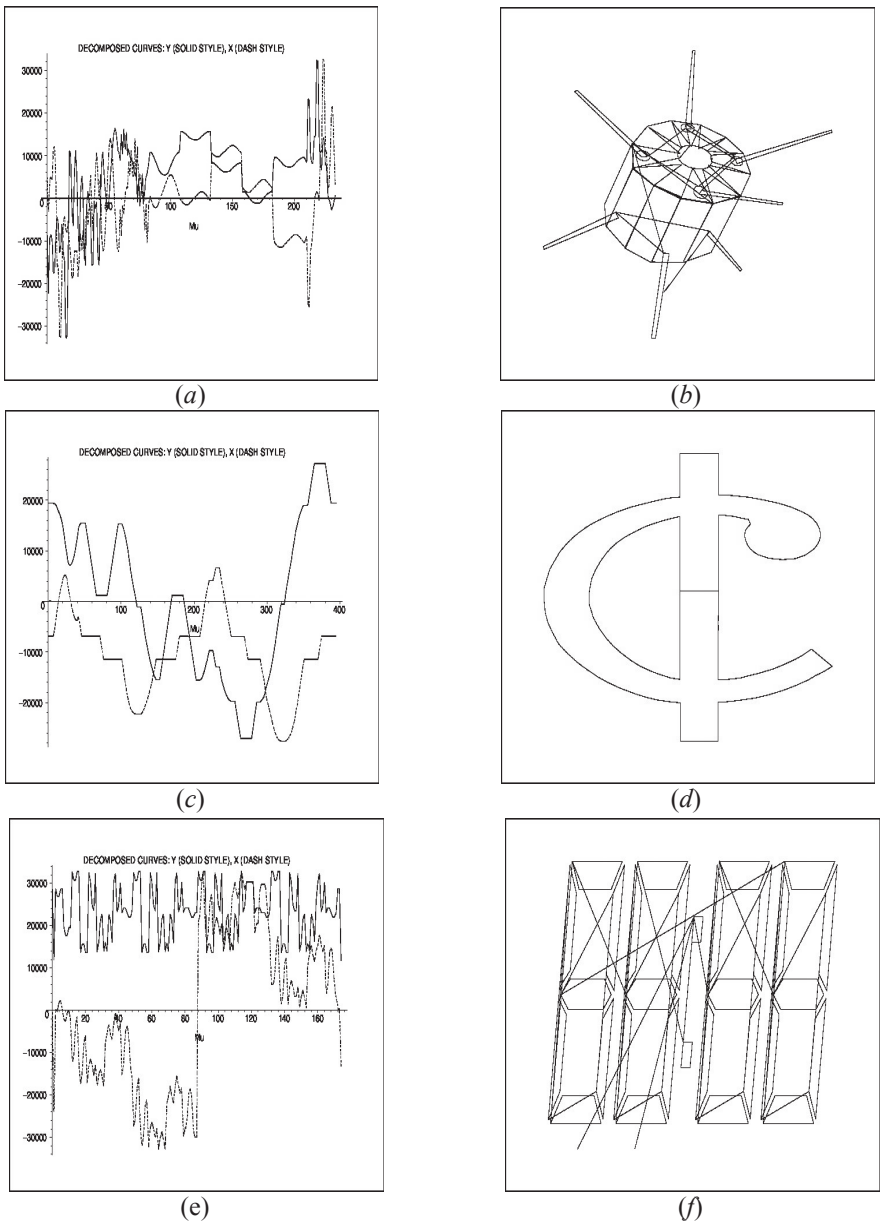

Figure 3 Free images taken from the SpectraScan™ website, (*a*) Decomposed Piecewise-Linear curves for Satellite, (*b*) Satellite plotting, (*c*) Decomposed Piecewise-Linear curves for Cent, (*d*) Cent plotting, (*e*) Decomposed Piecewise-Linear curves for Digital watch, (*f*) Digital watch plotting

Besides the computing aspects of memory and complexity, two features related to the performance of the Piecewise-Linear approach will now be discussed: sharpness in the drawing pattern and latency at the corners. In order to analyze these parameters, the satellite pattern in figure 4(*a*) is sketched using the SGMS and the LabView fixture. As can be seen in figure 4(*b*), the National Instruments cards were not fast enough to handle the 2136 points of the original test pattern, resulting in a sketch not visible even when using a camera with an aperture time of 1.2 seconds for the case of Point-oriented. For the Piecewise-Linear approach, the resulting sketch was fully visible using the same camera under the same configuration, as shown in figure 4(*c*).

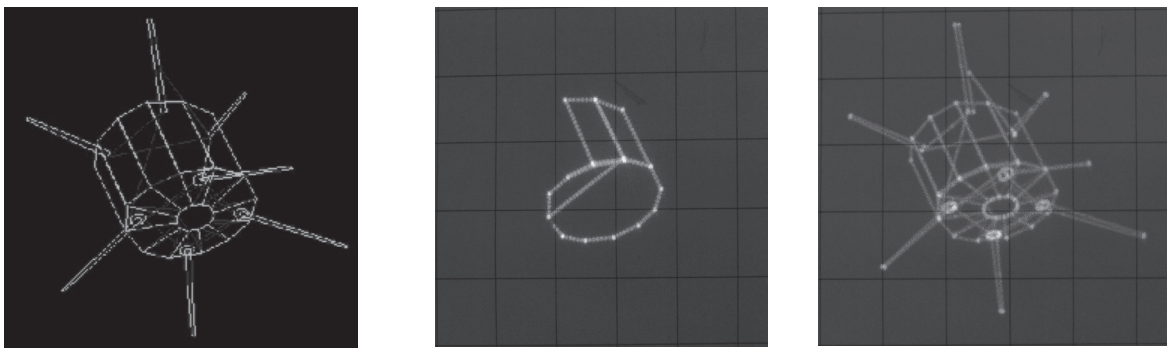

(*a*) (*b*) (*c*)

Figure 4 Satellite pattern sketching: (*a*) Original 2136-points image, (*b*) Point-oriented sketching, (*c*) Piecewise-Linear sketching

Thereby, from the above, it can be inferred that Piecewise-Linear requires much less computational resources than their point-oriented counterpart. To abide the previous problem, the satellite pattern is reduced to a 233 point file (Fig. 5(*a*)). In figure 5(*b*) an instantaneous capture of the satellite pattern using the Point-oriented strategy is shown. Additionally, the figure 5(*c*) shows the result obtained under the same conditions following the Piecewise-Linear strategy.

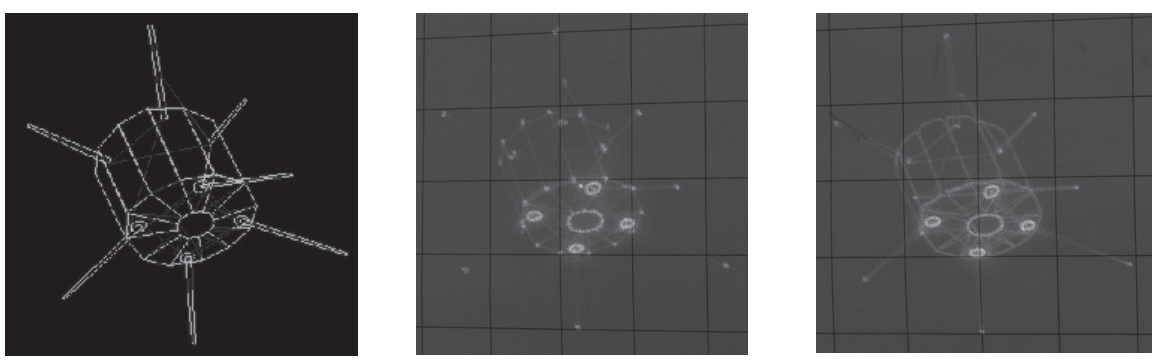

Figure 5 Satellite pattern sketching: (*a*) Original 233-points image, (*b*) Point-oriented sketching, (*c*) Piecewise-Linear sketching

As it can be seen from this comparative test, Piecewise-Linear provides a better sharpness at a less computational cost.

On the other hand, latency at the corners is a problem related to the inertia of the mechanic system at the moment in which their trajectory changes abruptly. To emphasize this problem, the triangle shown in figure 6(*a*) is sketched using Piecewise-Linear forcing the system to draw one side in one single stroke as it would be done in Vector-oriented. Thus, it can be seen from the magnification of the corner at figure 6(*b*) a ringing effect in the line projection. This effect is fully related to the inertia of the mechanical system of the SGMS. In order to overcome this problem, Piecewise-Linear does not trace lines in a single stroke, but with a sequence of points obtained from the evaluation of the set of parametric equations. Because of this, by evaluating the function several times to define a single trajectory, the number of evaluations among the different traces and at the corners augments, assuring a sharper projection and reducing the speed of the trace avoiding any problem as overshooting or ringing.

Conclusion

In this paper, a comparative study between methodologies for laser projection by using scanning galvanometer mirror systems was presented. As a result of the comparative study, it could be observed that the Piecewise-Linear methodology in comparison against the Point-based, exhibits attractive advantages such as: memory saving in the representation model, less requirement of hardware resources, greater processing speed, capability to overcome the problems of overshooting and ringing in laser projection by controlling the frequency of evaluation of the decomposed functions, and finally an improved sharpness for the projected curves. The Piecewise-Linear technique was succesfully applied to outline several patterns, showing its capability of sketching any curve. Now our ongoing work centers on exploring potential applications of the proposed technique and incorporate additional features to the SGMS such as the control of velocity in the laser beam as well as the laser intensity.

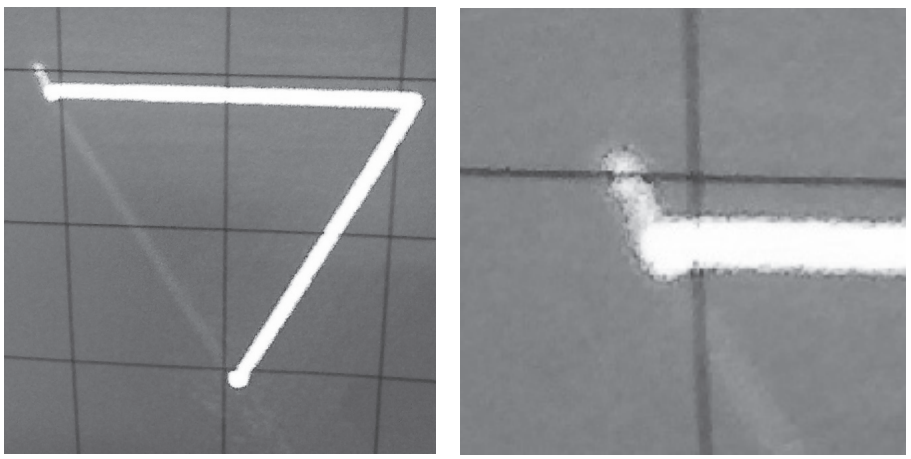

(a) (b)

Figure 6 Overshooting effect in the line projection: (*a*) Two-sides sketching of triangle, (*b*) Magnification of the corner

References

1. L. Meyer, N. Otberg, W. Sterry, J. Lademann. "In vivo confocal scanning laser microscopy: comparison of the reflectance and fluorescence mode by imaging human skin". *Journal of Biomedical Optics*. Vol. 11. 2006. pp. 1-7.

2. B. Vohnsen, D. Rativa. "Ultrasmall spot size scanning laser ophthalmoscopy". *Biomedical Optics Express*. Vol. 2. 2011. pp. 1597-1609.

3. M. Sridhar, S. Basu, V. Scranton, P. Campagnola. "Construction of a laser scanning microscope for multiphoton excited optical fabrication". *Rev. Sci. Instrum.* Vol. 74. 2003. pp. 3474–3477.

4. M. Chen, Y. Chen, W. Hsiao, S. Wu, C. Hu, Z. Gu. "A scribing laser marking system using DSP controller". *Optics and Lasers in Engineering*. Vol. 46. pp. 410-418.

5. F. Blais. "Review of 20 Years of Range Sensor Development". *Journal of Electronic Imaging*. Vol. 13. 2004. pp. 231-243.

6. RP Photonics. *Encyclopedia of Laser Physics and Technology*. Available on: http://www.rp-photonics.com/laser_applications.html?s=ak Accessed: July 27, 2014.

7. THORLABS. *Thorlabs Small Beam Diameter Scanning Galvo Mirror Systems*. Available on: http://www.thorlabs.de/newgrouppage9.cfm?objectgroup_id=3770 Accessed: July 27, 2014.

8. Edmund Optics. *Dual Axis Galvanometer Optical Scanners*. Available on: http://www.edmundoptics.com/electro-optics/electro-optics-accessories/dual-axis-galvanometer-optical-scanners/2717 Accessed: July 27, 2014.

9. F. Menendez, O. Halabi, N. Chiba. *Vector-based library for displaying Bezier curves using a laser projector*. Proceedings of the IWAIT 07. Bangkok, Thailand. 2007. pp. 121-126.

10. P. Abderyim, F. Menendez, O. Halabi, N. Chiba. *Morphing-based vectorized candle animation for laser graphics*. Proceedings of the IWAIT 07. Bangkok, Thailand. 2007. pp.127-132.

11. Technoroam. *Laser Scanner: Experiment 28*. http://www.technoroam.sk/lasershow/downloads/ENP28.pdf Accessed: July 27, 2014.

12. Lasershow Laser Systems. *TraceIT: free bitmap tracer for LD2000 and FB3*. Available on: http://www.pangolin.com/LA_Studio/TraceIT.htm#TraceIT%20and%20Pangolin%20Lasershow%20Designer%202000 Accessed: July 27, 2014.

13. SOLLINGER. *Basic Laser Projectors*. Available on: http://www.laseranimation.com/en/products/laser-systems Accessed: July 27, 2014.

14. PHOENIX. *Phoenix4 PRO/PROplus.* Available on: http://www.phoenix-showcontroller.de/en/phoenix/pro-en/ Accessed: July 27, 2014.

15. Medialas. *Mamba Elements*. Available on: http://www.medialas-showlaser.de/mamba_elements.html?&L=1 Accessed: July 27, 2014.

16. GSI. *Laser Products: Beam Delivery Technologies*. Available on: http://www.gsig.com/Laser-Products Accessed: July 27, 2014.

17. LOBO. *Projectors.* Available on: http://www.lobo.de/index.php?id=lasershow_products&L=1&maincat_uid=14&subcat_uid=0 Accessed: July 27, 2014.

18. O. Halabi, N. Chiba. "Effcient vector-oriented graphic drawing method for laser-scanned display". *Elsevier Displays*. Vol. 30. 2009. pp. 97-106.

19. V. Jimenez, H. Cerecedo, H. Vazquez, L. Beltran, U. Filobello. "A parametric piecewise-linear approach to laser projection". *Computational and Applied Mathematics*. DOI:10.1007/s40314-013-0099-2. 2013. pp. 1-21.

20. L. Chua, A. Deng. "Canonical piecewise-linear modeling". *IEEE Transactions on Circuits and Systems*. Vol. 33. 1986. pp. 511-525.

21. L. Chua, A. Deng. "Canonical piecewise-linear representation". *IEEE Transactions on Circuits and Systems*. Vol. 35. 1988. pp. 101-111.

22. S. Kang, L. Chua. "A global representation of multidimensional piecewise-linear functions with linear partitions". *IEEE Transactions on Circuits and Systems*. Vol. 25. 1978. pp. 938-940.

23. S. Kang, L. Chua. "Section-wise piecewise-linear functions: Canonical representation, properties and applications". *IEEE*. Vol. 65. 1977. pp. 915-929.

24. V. Jimenez, L. Hernandez, A. Sarmiento. *Decomposed Piecewise-Linear Models by Hyperplanes Unbending*. Proceedings of the IEEE International Symposium on Circuits and Systems. Island of Kos, Greece, 2006. pp. 2353-2356.

25. V. Jimenez. *Decomposed Piecewise-Linear Representation Applied to DC Analysis*. PhD Thesis, Instituto Nacional de Astrofísica, Óptica y Electrónica. Puebla, México. 2006. pp. 47-68.

26. V. Jimenez, E. Muñoz, H. Vazquez, J. Chavez, L. Hernandez, L. Sarmiento, M. Cerdan. "A Piecewise-Linear Fitting Technique for Multivalued Two-dimensional Paths". *Journal of Applied Research and Technology*. Vol. 11. 2013. pp. 636-640.

27. LASERPHOTO. *LP20 Galvanometer Based Optical Scanner.* Available on: http://www.laserphoto.org/en/pic/digi/20085510211232.pdf Accessed: July 27, 2014.

28. SpectraScan. *Samples-Software Downloads* Avilable on: http://www.lasershs.com/Sample_Download.htm Accessed: July 27, 2014.